

The near-field characteristics of the Perth Seawater Desalination Plant discharge

Final report

P. Okely, J.P. Antenucci, C.L. Marti and J. Imberger

December 2007

Centre for Water Research



The University of Western Australia, M023, 35 Stirling Hwy, Nedlands, Western Australia 6009

Phone 61 8 6488 2410 **Fax** 61 8 6488 3053 **Email** services@cwr.uwa.edu.au

Web <http://www.cwr.uwa.edu.au>

Executive Summary

This report details the results of a field experiment conducted to investigate the near-field flow characteristics of a hypersaline brine generated by the Perth desalination plant that is discharged into Cockburn Sound, Western Australia via an offshore diffuser. The key objective was to determine the dilution of the negatively buoyant plume as it exited the diffuser under three different discharge regimes (1/3, 2/3 and full capacity), and to relate these measurements to scaling arguments derived from laboratory measurements

Equations based on the densimetric Froude number $F = U / \sqrt{g_0' d}$, where U is the discharge jet velocity, d is the nozzle diameter and g_0' is the reduced gravity due to the density difference between the ambient water and the discharge salinity, were found to adequately describe the thickness of the resulting saline layer and the dilution of the brine for $F > 20$, as in the laboratory. For $F < 20$, dilution was greater than anticipated based on extrapolation of the laboratory results.. Dilution was greater than 45 times (the design dilution) at 50 metres from the diffuser for all flow rates: 54 times for 1/3 flow, 59.5 times for 2/3 flow and 61.4 times for full flow.



CERTIFICATE OF APPROVAL FOR ISSUING CWR DOCUMENTS

DOCUMENT AND PROJECT DETAILS:

Document title: The near-field characteristics of the Perth Seawater Desalination Plant discharge – Final Report

Document no. (ED, WP): WP2175PO

Document author(s): Okely, P., Antenucci J.P., Marti, C.L. and Imberger, J.

Project title: Cockburn Sound Modelling Project

Project manager: Jason Antenucci

Client organisation: Water Corporation

Client contact: David Luketina

Synopsis: Final Report

REVISION AND DISTRIBUTION HISTORY:

Issue	Issued to	Qty	Date	Reviewed	Approved
Draft	Authors		03/12/2007	Hillmer	
Draft	Authors		03/12/2007	Yeates	
Draft	Client		10/12/2007		Antenucci
Final	Client		10/13/2007		Antenucci
Revised	Client		07/04/2008	Marti	Antenucci

RELEASE STATUS:

Confidential: Yes

© Copyright: Centre for Water Research (CWR)

TABLE OF CONTENTS

Executive Summary	2
1 Introduction	5
2 Methodology	6
2.1 Overview	6
2.2 Instrumentation.....	6
2.2.1 Fine-scale Profiler (F-probe)	6
2.2.2 Acoustic Doppler Current Profiler (ADCP).....	7
2.2.3 Lake Diagnostic System (LDS)	8
2.3 Field Programme.....	9
3 Meteorology	10
4 Brine Discharge	11
5 Near-field Characteristics	11
5.1 Introduction	11
5.2 Field experiment results	14
6 Summary	21
7 Conclusions	24
8 References	25

1 Introduction

The Perth Seawater Desalination Plant is located on the eastern shore of Cockburn Sound, a coastal embayment south of Fremantle, Western Australia. The plant is designed to produce 45GL of potable water per year via reverse osmosis. This desalination process is approximately 45% efficient, thus the hypersaline discharge returned to the Sound is estimated to have a salinity of approximately 63 ppt, with the salinity of the ambient receiving waters approximately 35 ppt. The saline discharge enters the Sound via a diffuser which is designed to reduce the salinity to 1ppt above ambient concentrations within 50 metres of the diffuser.

The diffuser is located around 500 metres from shore and is 160 metres long, running perpendicular to the shore along the seabed, with 40 evenly spaced ports. Each port consists of pipe that extends 1 metre vertically from the seabed with the nozzle inclined at 30° from the vertical. This inclination has been shown to approximately double the dilution relative to a vertically-oriented nozzle (Roberts and Toms 1987). The internal diameter at the port exit is 0.130 metres, and the full flow rate per port is 40 L/s.

This report details measurements made to determine the near-field characteristics of the saline plume, in particular the terminal height of rise and the final saline layer thickness and dilution. Measurements were made within 50 - 100 metres of the diffuser under three different discharge regimes to quantify the impact of the discharge on the plume formed in Cockburn Sound.

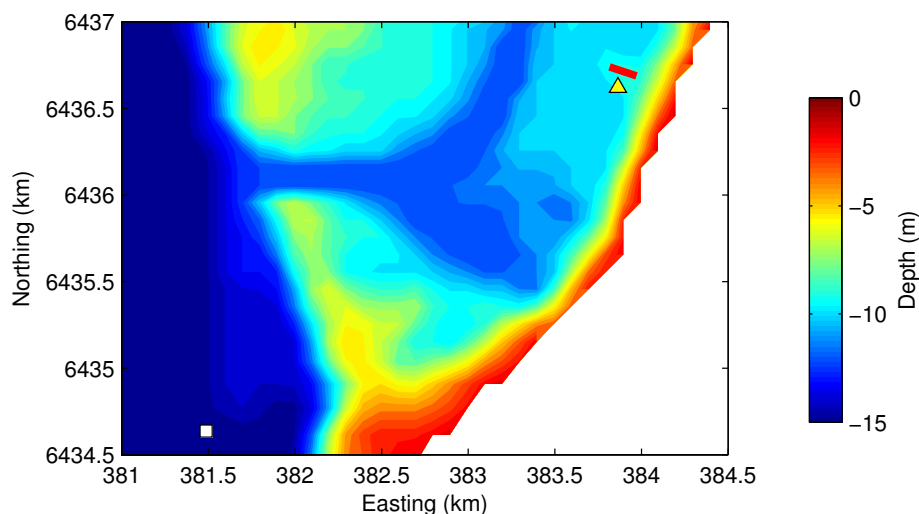


Figure 1.1. Perth Seawater Desalination Plant diffuser location (red line) and coastal bathymetry. The location of the bottom-mounted ADCP is shown by the triangular marker, and the location of the LDS station, measuring meteorological variables, water temperature and conductivity, is marked by the open square.

2 Methodology

2.1 Overview

The field investigation was undertaken on three days with different discharge flow rates: one-third full flow capacity on 25 Oct, two-thirds full flow capacity on 26 Oct, and full flow capacity on 6 Nov 2007. Measurements consisted of high spatial and temporal resolution Conductivity-Temperature-Dissolved Oxygen (CTD) profiling using a fine-scale profiler (F-probe), water velocities measured using a bottom moored SonTEK Acoustic Doppler Current Profiler (ADCP), and meteorological variables from the moored Lake Diagnostic System (LDS).

Note that, on the last experiment day (6 Nov) Western Australian daylight savings time was in effect (AWDST); *however, all times referenced in this report are in AWST.*

2.2 Instrumentation

2.2.1 Fine-scale Profiler (F-probe)

On profiling days, a fine-scale profiler (F-probe) was deployed measuring:

- Temperature
- Conductivity
- Depth
- pH
- dissolved oxygen
- turbidity

The sensor accuracy of each of these sensors is shown in Table 2.1. The profiler was deployed in free-falling mode, collecting data at a rate of 50 Hz with a drop velocity of 0.5 m s^{-1} . This yielded a vertical resolution of 1 cm. Only measurements of salinity are used in this report as salinity dilution is indicative of the diffuser performance.

Table 2.1. Sensor accuracy of F-probe

Sensor	Range	Resolution	Time Response	RMS Noise	Accuracy (Better than)
Depth	0 - 60 m	1.3×10^{-5} m	-	0.004 m	0.01%
Temperature	5 - 30 °C	8.4×10^{-7} °C @ 0 °C, 1.05×10^{-6} °C @ 30 °C	72 ms @ 1m/s, 84ms @ 0.5m/s	0.001 °C	0.001 °C
Conductivity	0 - 6 S/m	1.64×10^{-8} S/m @ 0 S/m 2.5×10^{-7} S/m @ 6 S/m	70 ms @ 1m/s, 85ms @ 0.5m/s	0.0001 S/m	0.001 S/m
Dissolved Oxygen	0 - 15 ml/l	0.01 ml/l	-	-	0.1 ml/l
pH	0 - 14 pH units	0.01 pH units	-	-	0.05 pH units
Turbidity	0.04 - 100 FTU	0.015 FTU	-	-	0.1 FTU + 3%

2.2.2 Acoustic Doppler Current Profiler (ADCP)

A 1500kHz Sontek ADCP measuring water velocity was bottom mounted approximately 100 m south of the diffuser at 32° 12' 03.40" S and 115° 46' 04.30" E (Figure 1). The ADCP configuration used is shown in Table 2.2.

Table 2.2. ADCP settings for the three experiments.

Configuration Parameter	Parameter Value
Cell Size	0.25 m
Number of Cells	50
Blanking Distance	0.15 m
Maximum Profiling Range	12.65 m
Averaging Interval	300 sec
Profile Interval	360 sec
Accuracy	±1% of measured velocity

2.2.3 Lake Diagnostic System (LDS)

An LDS was installed at 32° 13' 08.15" S and 115° 44' 31.50" E on September 12 2007 (Figure 1.1). The LDS consisted of a full meteorological station measuring

- air temperature
- relative humidity
- wind speed
- wind direction
- shortwave radiation
- net radiation

at 1.5 metres above the surface, as well as a set of underwater sensors measuring water temperature (10 sensors at 0.25, 0.5, 0.75, 1, 2, 5, 8, 11 m from the surface and at 3 and 2 m above the bottom), water depth, and conductivity (2 sensors at 1 m from the surface and 0.7 m above the bottom). The water depth ranges between 15 and 16 m. The sampling interval was 30 seconds.

2.3 Field Programme

The ADCP and F-Probe deployment schedule is shown in Table 2.3. F-probe profile locations are shown in Section 5.2.

Table 2.3. Field study programme for the three experiments.

Time	Method	Flow rate	Description
24/10/07 11:42	ADCP		Instrument installed approximately 100 m south of the diffuser.
25/10/07 07:21-11:02	F-probe	1/3	Profiling in S-N transects across diffuser.
26/10/07 06:45-08:46	F-probe	2/3	Profiling in S-N transects across diffuser.
26/11/07 08:50	ADCP		Instrument removed.
06/11/07 06:49	ADCP		Instrument installed approximately 100 m south of the diffuser.
06/11/07 07:06-11:25	F-probe	3/3	Profiling in S-N transects across diffuser.
06/11/07 08:40-09:06	F-probe	3/3	Anchored 50 m north of centre of diffuser.
06/11/07 09:17-09:42	F-probe	3/3	Anchored 100 m north of centre of diffuser.
06/11/07 12:40	ADCP		Instrument removed.

3 Meteorology

Meteorological conditions measured in Cockburn Sound during the three sampling dates are shown in Figure 3.1. The first sampling day (25 Oct 2007) was characterised by a strong northerly wind blowing at approximately 7 m s^{-1} , clear skies and increasing temperatures as the sampling progressed. Sampling on the second day (26 Oct 2007) was ahead of a large storm event, with winds also around 7 m s^{-1} , but from the west. Sampling ceased as the weather conditions deteriorated due to the approaching storm. The third day (6 Nov 2007) was characterised by south south-westerly winds blowing at approximately 6 m s^{-1} and mostly clear skies. The water temperature cooled between sampling events 2 and 3, but remained in the range of $18.5 - 19.5 \text{ }^\circ\text{C}$. The water column was well-mixed to weakly stratified, and was typical of previous measurements made in the Sound.

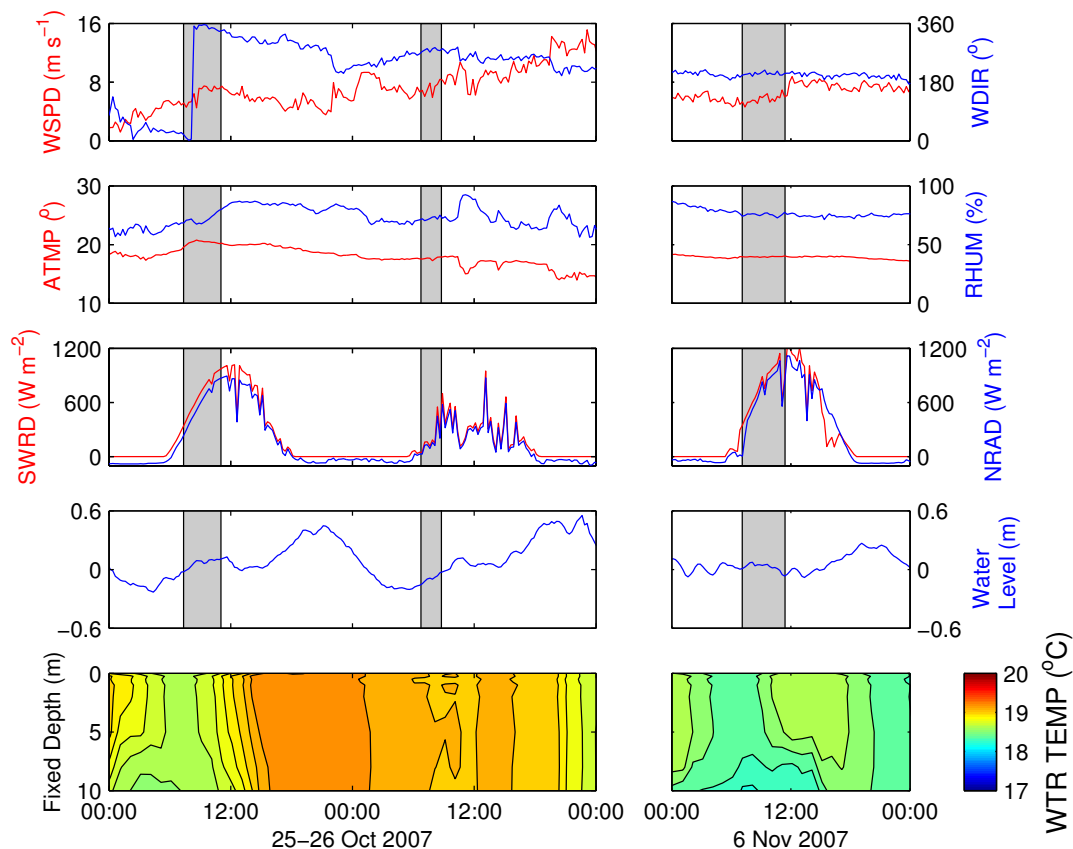


Figure 3.1. Meteorological parameters and water column temperature measured by the LDS during the two field study periods (shading indicates profiling periods, contours at $0.1 \text{ }^\circ\text{C}$ in bottom panel). WSPD – wind speed. WDIR – wind direction. ATMP – air temperature. RHUM – relative humidity. SWRD – shortwave radiation. NRAD – net radiation. WTR TEMP – water temperature.

4 Brine Discharge

Discharge characteristics for the desalination plant during the three experiments are shown in Table 4.1.

Table 4.1. Desalination Plant discharge characteristics during the three experiments.

	25 Oct 2007 - 1/3 flow	26 Oct 2007 - 2/3 flow	6 Nov 2007 - 3/3 flow
Flow Rate ($\text{m}^3 \text{s}^{-1}$)	0.64	1.43	2.19
Salinity (psu)	56.0	67.3	66.9
Temperature ($^{\circ}\text{C}$)	19.8	20.5	20.3

5 Near-field Characteristics

5.1 Introduction

The basic characteristics of an inclined, dense jet are presented in Figure 5.1, depicting the terminal height of rise of the jet (y_t), the height of the bottom layer (y_L), the distance of the impact point (x_i), the distance to the edge of the mixing zone (x_m), the dilution at the impact point (S_i) and the dilution at the edge of the mixing zone (S_m). The dense plume rises into the ambient fluid as a jet, entrains ambient fluid until it reaches a terminal height, then falls back to the bottom and entrains additional fluid on descent. Upon impact with the bottom, the plume spreads laterally, further entraining fluid from above until reaching the edge of the mixing zone.

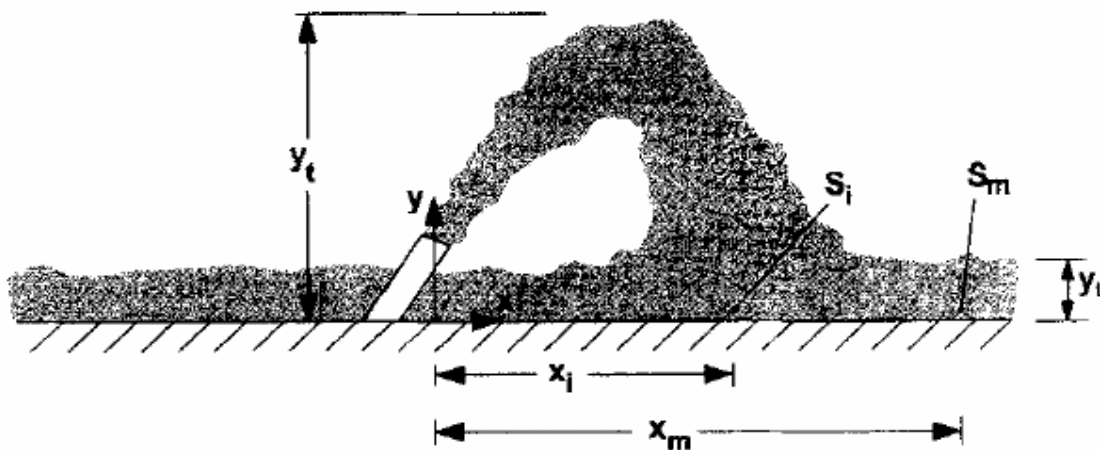


Figure 5.1. Definition diagram for an inclined dense jet (Roberts et al. 1997).

Laboratory results by Roberts et al. (1997) showed that dilution of a negatively buoyant jet (Figure 5.1) scaled with the densimetric Froude number $F = U / \sqrt{g_0' d}$, where U is the discharge jet

velocity, d is the nozzle diameter and $g'_0 = g(\rho_d - \rho_a)/\rho_a$ is the reduced gravity due to the density difference between the ambient water (ρ_a) and the discharge (ρ_d). For the three experiments, the Froude number was calculated and is presented in Table 5.1. Note that the results of Roberts et al. (1997) apply only to $F \geq 20$. The density of the ambient water was taken as the average density of the upper 5 metres of the water column.

The background conditions into which the brine is discharging are unsteady, with wind and tides generating variable currents (Figure 5.2). During the 1/3 flow experiment, the prevailing northerly wind generated currents to the south, although currents in the bottom 7 metres of the water column were to the north (Figure 5.2). During the second experiment the current velocities were very low ($\sim 2 \text{ cm s}^{-1}$), and were highest during the third experiment ($\sim 6 \text{ cm s}^{-1}$). The effects of an ambient cross-flow on negatively buoyant jets was investigated by Roberts and Tom (1987), who define an ambient flow Froude number $F_a = U_a / \sqrt{g'_0 d}$ where U_a is the ambient current velocity. For $F_a \ll 1$, no effects of the ambient current should be observed. For the three experiments, F_a was approximately 0.28, 0.11 and 0.35, respectively. This suggests that the strongest signal of the cross-flow should be observed in the full flow case, and may also be observed for the 1/3 flow.

Table 5.1. Densimetric Froude number (F) calculations for the three flow rates, along with calculations of the ambient flow Froude number.

	1/3 flow	2/3 flow	3/3 flow
$Q_{\text{total}} (\text{m}^3 \text{ s}^{-1})$	0.641	1.435	2.185
$Q_{\text{per port}} (\text{m}^3 \text{ s}^{-1})$	0.016	0.036	0.055
$U (\text{m s}^{-1})$	1.208	2.70	4.116
$\rho_{\text{discharge}}$	1040.96	1049.47	1049.21
$\rho_{\text{background}}$	1024.85	1024.80	1025.20
g'	0.154	0.236	0.230
F	8.53	15.4	23.8
$U_a (\text{m s}^{-1})$	0.04	0.02	0.06
F_a	0.28	0.11	0.35

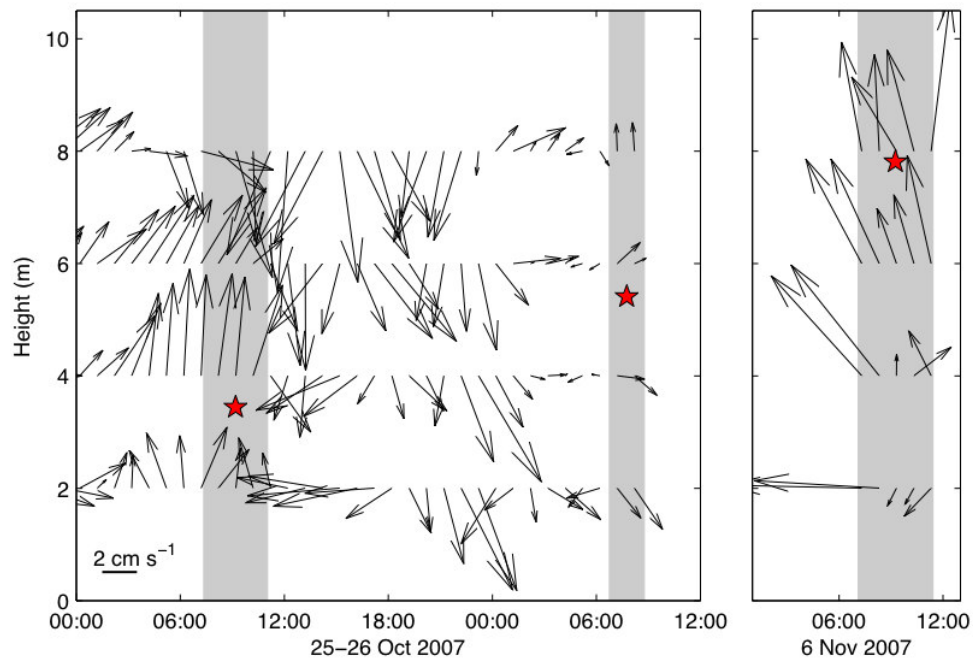


Figure 5.2. Water column velocities measured by the ADCP during the three field study periods (shading indicates profiling periods). Horizontal velocities averaged hourly and across height ranges 1-3, 3-5, 5-7 and 7-9 m are shown as vectors with North corresponding to top of page (scale is included in bottom left corner of left panel). The red star markers (★) indicate the terminal height of rise of the jet for each sampling period, and so the jet will feel the effects of the velocities below this level.

5.2 Field experiment results

Based on the scaling results of Robert et al. (1997) and the Froude number calculations presented above, the expected dilution and mixing characteristics were computed and are presented in Table 5.2.

Table 5.2. Plume characteristics based on scaling of Roberts et al. (1997) for the three flow rates, where F is the densitmetric Froude number and d is the port diameter. Note that one metre has been added to the calculation of the terminal height of rise as the ports protrude this distance above the sea bed.

	Scaling equation	1/3 flow	2/3 flow	3/3 flow
Dilution at impact	1.6F ($\pm 12\%$)	13.6	24.7	38.1
Dilution at mixing zone edge	2.6F ($\pm 15\%$)	22.2	40.0	61.9
Terminal height of rise [m]	2.2Fd	3.44	5.41	7.81
Location of impact point [m]	2.4Fd	2.66	4.81	7.43
Length of mixing zone [m]	9Fd	10.0	18.0	27.9
Thickness of bottom layer [m]	0.7Fd	0.78	1.40	2.17

In order to investigate the near-field dilution dynamics, the lower layer thickness was obtained by determining the point in each profile where the change in salinity over a 0.1 m interval exceeded 0.05 psu. Figure 5.3 shows some sample profiles from the second experiment: a red circle marks the top of the layer as determined by the salinity gradient.

For the 1/3 flow case, the maximum height of rise of the plume measured was typically 4 metres but reached up to 8 metres from the bed on one occasion (Figure 5.4). The plume formed a layer approximately 2 metres thick, with dilution slightly less at 50 metres distance to the north of the diffuser (40-60 times rather than 60-80 times to the south) (Figure 5.4). The predicted terminal height of rise of the plume was 3.5 metres, and so the rising jet experienced currents of up to 4 cm s⁻¹ (Figure 5.2). The scaling analysis of Roberts and Toms (1987) and Roberts et al. (1997) must be applied to this flow rate with caution as $F < 20$.

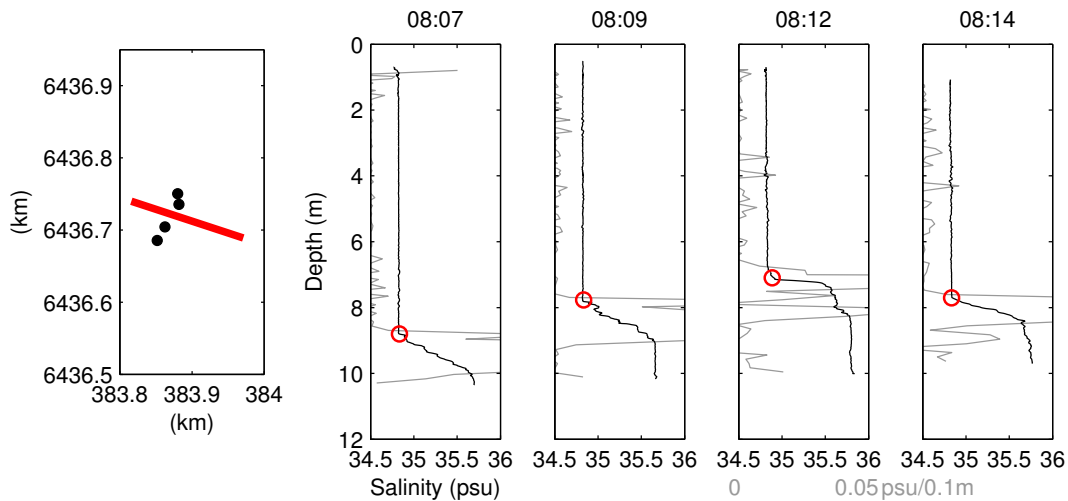


Figure 5.3. Salinity profiles from a S-N transect across the diffuser on 26 Oct 2007 (at times shown above profile panels). Left panel shows location of profiles (circles) and diffuser (red line). The salinity data collected by the fine-scale profiler is shown in black in the profile panels. The grey line shows the salinity gradient, determined as change in salinity over 0.1 m intervals, and the red circles show where the salinity gradient exceeded 0.05 psu / 0.1 m (corresponding to the right-hand limit of the x-axis).

For the 2/3 flow case, the maximum height of rise of the plume measured was approximately 5 metres from the bed (Figure 5.5), similar to the terminal height of rise predicted from Roberts et al. (1997) of 5.4 metres. The plume formed a layer approximately 2 metres thick, with similar dilution both to the north and south of the diffuser (40-60 times at 50 metres). The prevailing wind direction at the time was from the west, with low currents ($\sim 2 \text{ cm s}^{-1}$). The Froude number was approximately 15, and so the scaling of Roberts and Toms (1987) and Roberts et al (1997) should be applied *a-priori* with caution. As expected, no north-south variation in dilution was observed for the weak current conditions (Figure 5.5).

For the full flow case, the maximum height of rise of the plume measured was approximately 9 metres from the bed (Figure 5.6), similar to the terminal height of rise predicted from Roberts et al (1997). The plume formed a layer approximately 2.5 metres thick. The prevailing wind direction at the time was from the south-southwest, with current velocities to the north at 6 cm s^{-1} (Figure 5.6). The plume was pushed to the north, and at 50 metres the dilution was greater to the north (and the saline layer thicker) than to the south. This agrees with Roberts and Toms (1987) who showed that a jet in the direction of ambient current is diluted to a greater extent than jets opposed to the ambient current direction.

Dilution characteristics were averaged into 5 metre bins with distance from the diffuser and are presented in Figure 5.7 - Figure 5.9. It is clear from the data that the dilution at 50 metres from the

diffuser is greater than 40 times for all flow rates. The final layer thickness also corresponds well with those predicted by Roberts et al. (1997).

As an indication of the variability in the layer thickness and dilution over time, a series of anchored profiles were taken during the full flow experiment at 50 and 100 metres from the diffuser (Figure 5.10). The mean layer thickness for 50 and 100 metres was 3.6 metres and 3.0 metres with a standard deviation of 0.6 and 0.6 metres, respectively. The dilution for 50 and 100 metres was 64 times for both cases with a standard deviation of 10 and 12 times, respectively.

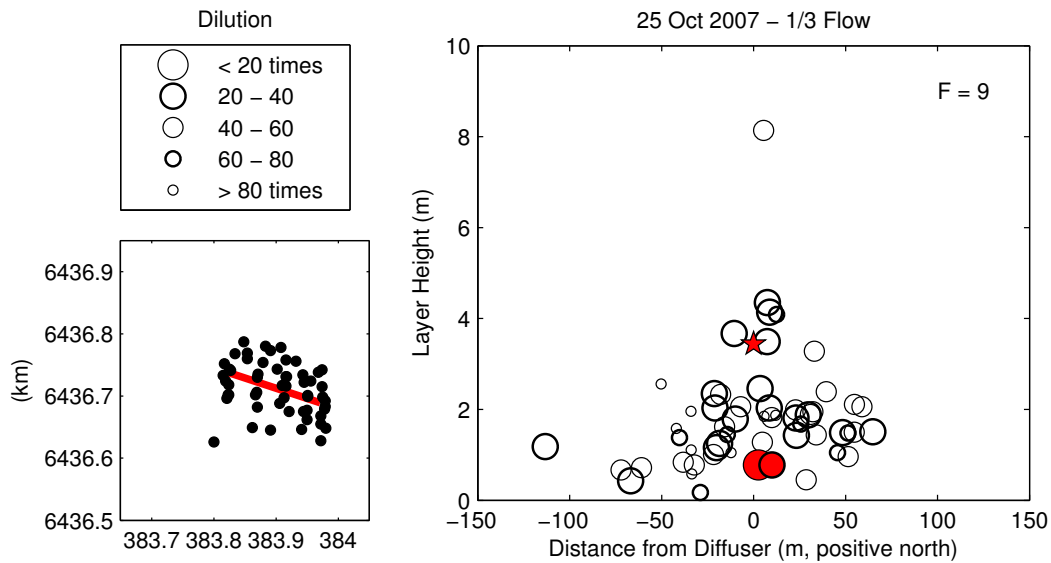


Figure 5.4. Saline discharge layer characteristics from profiles taken on 25 Oct 2007 during the one-third flow rate conditions. Bottom left panel shows locations of profiles. Right panel shows height of saline discharge layer in profile as a function of perpendicular distance from the diffuser. Circle size indicates dilution of discharge as calculated from overlying salinity, mean salinity of layer and salinity of raw discharge. Red symbols indicate theoretical estimates using jet-densimetric Froude number (top right corner of right panel) from Roberts et al (1997) of terminal height of rise of discharge (star), location and dilution at impact point and edge of mixing zone (circles).

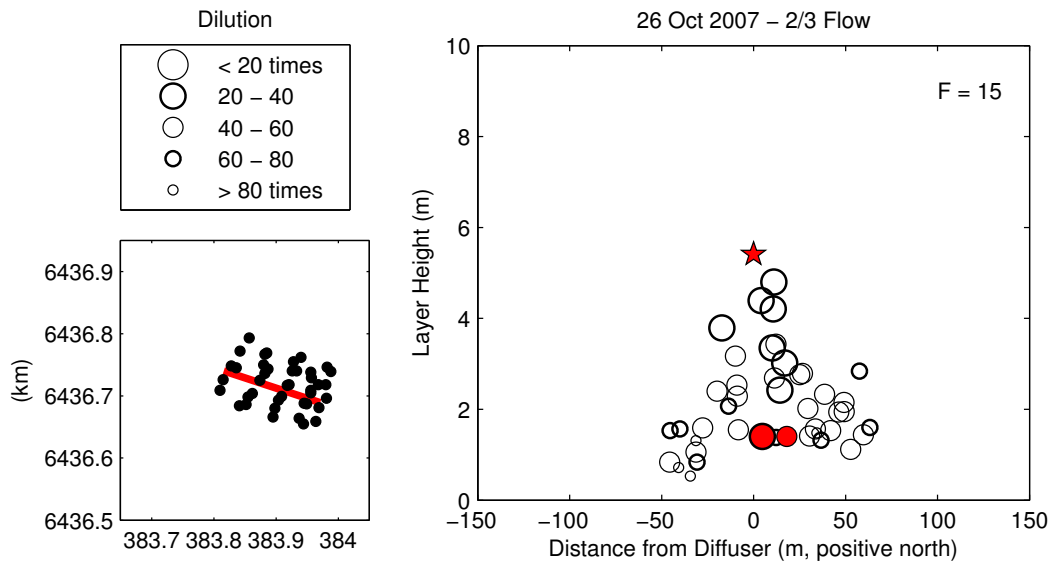


Figure 5.5. As for Figure 5.4, but for two-thirds flow rate on 26 Oct 2007.

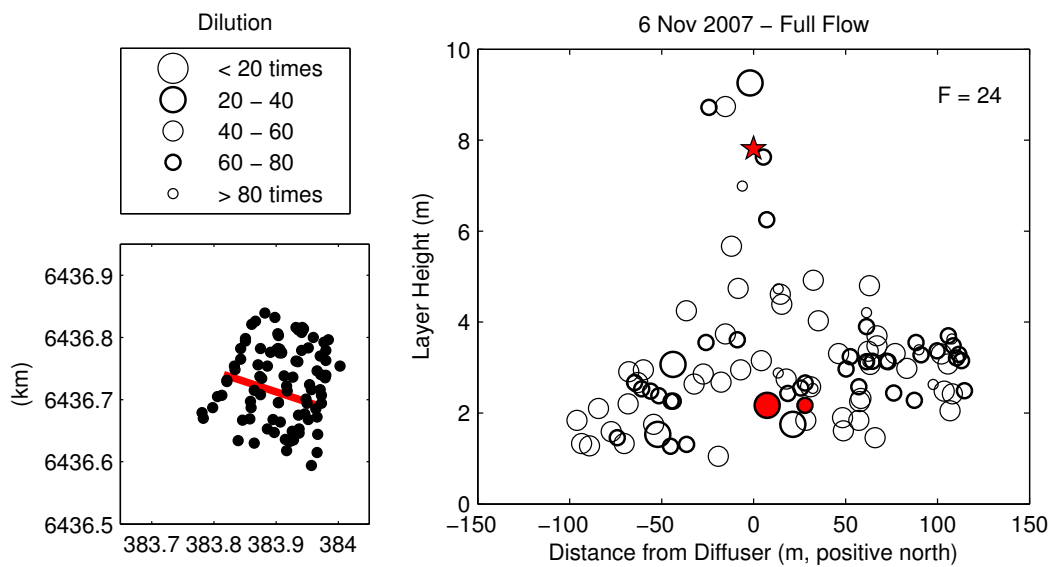


Figure 5.6. As for Figure 5.4, but for full flow rate on 6 Nov 2007.

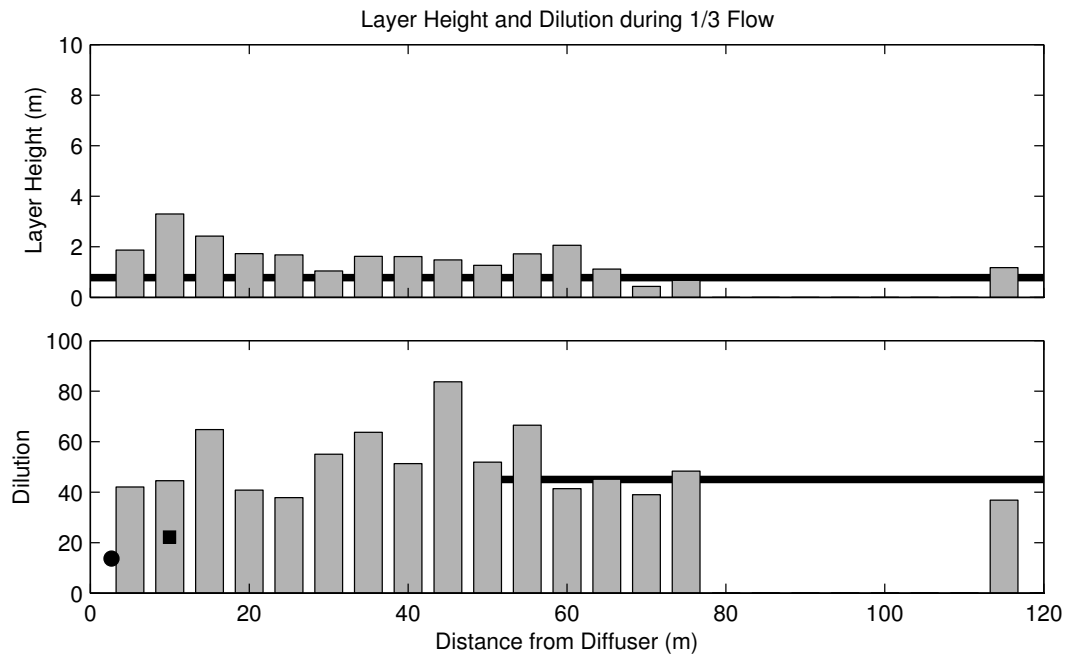


Figure 5.7. Ensemble average of saline discharge layer height (top panel) and dilution (bottom panel) for bins corresponding to 5 m intervals away from diffuser for 1/3 flow. Horizontal line in background of top panel show theoretical layer thickness from Roberts et al. (1997). Symbols in bottom panel show location and dilution at impact point (circle) and edge of mixing zone (square) predicted by Roberts et al. (1997). The horizontal line on the bottom panel represents the design target dilution of 45 times (marked from 50 metres from the diffuser onwards).

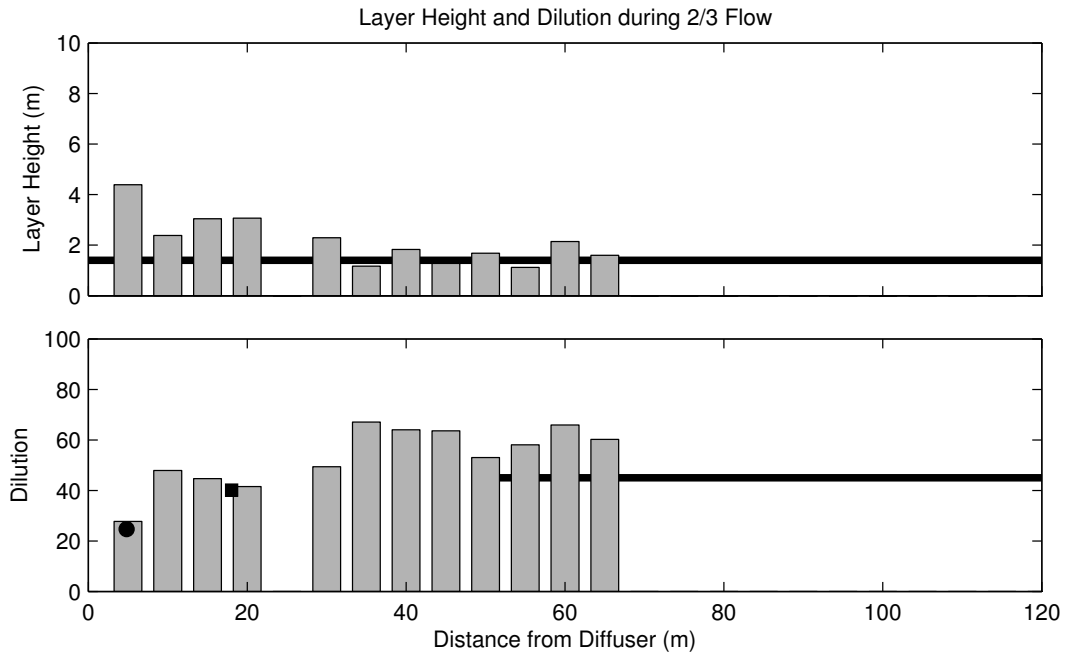


Figure 5.8. As for Figure 5.7, for 2/3 flow.

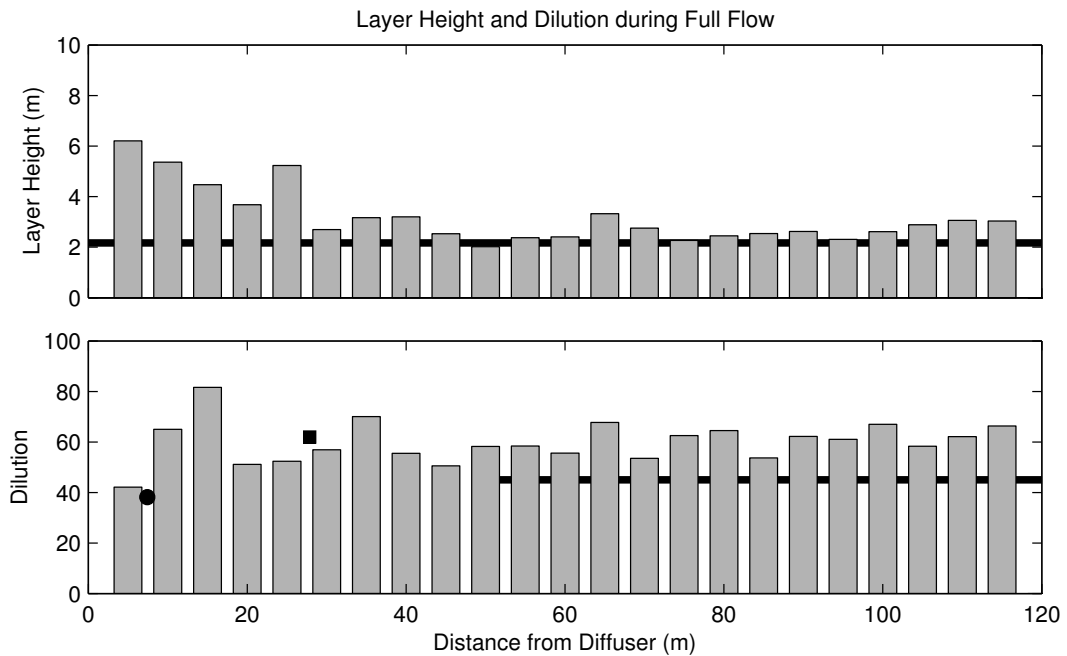


Figure 5.9. As for Figure 5.7, for full flow.

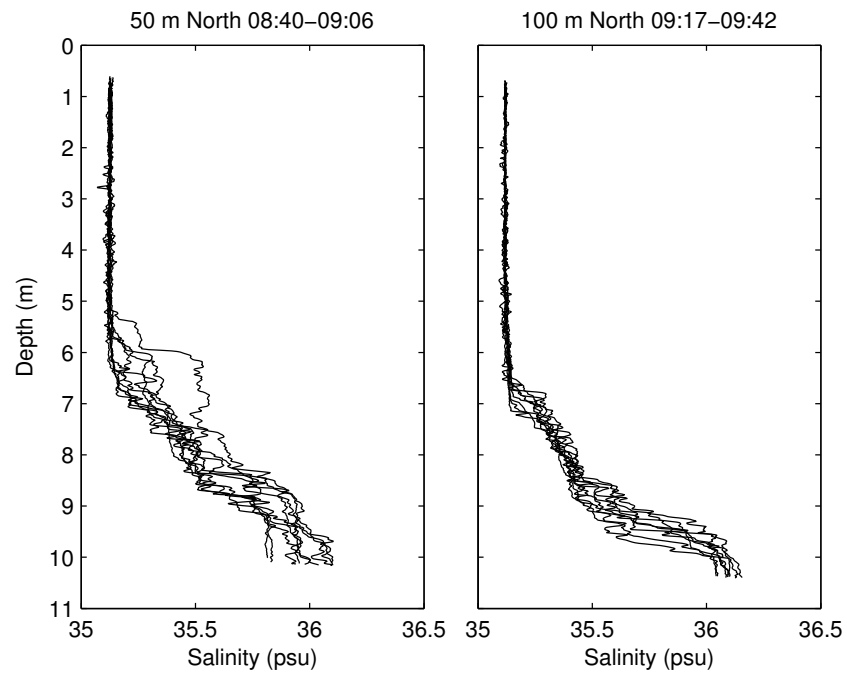


Figure 5.10. Salinity profile data collected while anchored 50 m and 100 m north of the centre of the diffuser on 6 Nov 2007.

6 Summary

The above results are summarised in Figure 6.1 and Figure 6.2. Figure 6.1 compares the dilution (D) (divided by the Froude number F) with the non-dimensional distance x/dF . This is directly comparable to Figure 5 from Roberts et al. (1997), where those authors found

$$\frac{D}{F} = C_3 = 2.6 \quad (1)$$

for $F > 20$. The measured mean dilution for $F > 20$ (the full flow condition, lowest panel) at the edge of mixing zone shows remarkable agreement with the dilution estimate derived in the laboratory, in fact to the same decimal place ($C_3 = 2.6$). For lower Froude numbers, dilution was found to be greater than that determined by extrapolating the results of Roberts et al. (1997) to $F < 20$.

This is shown clearly in Figure 6.2, where the mean dilution at the end of the mixing zone exceeded 50 in all cases (54 for the 1/3 flow, 59.5 for the 2/3 flow, and 61.4 for the full flow).

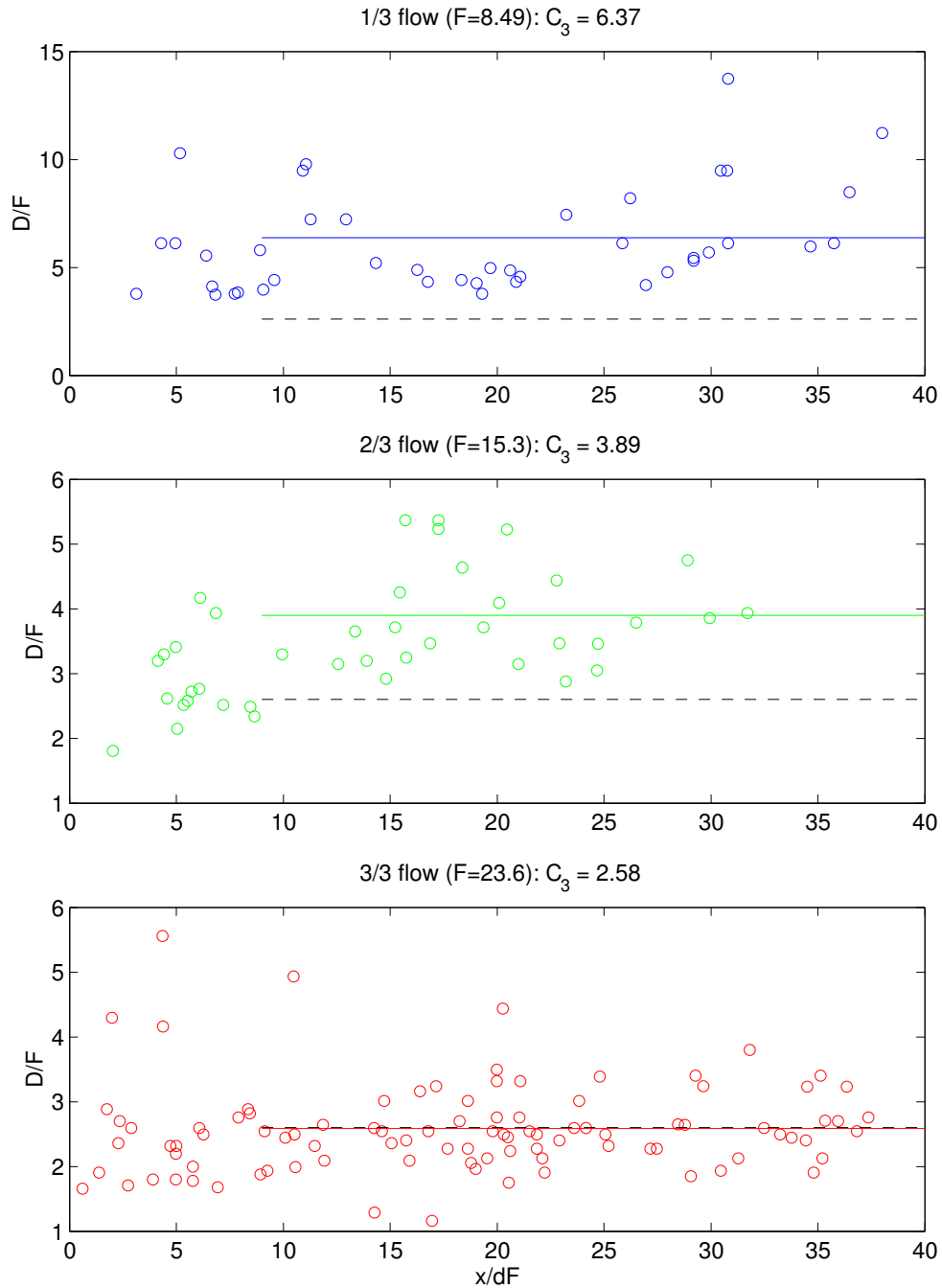


Figure 6.1. Dilution (D) divided by Froude number (F), plotted against non-dimensional distance from the plume source x/dF , for the three flow rates. The symbols represent the dilution determined from an individual profile, the solid line of the same colour represents the mean dilution for distances greater than $x/dF = 9$, and the black dashed line represents the results from Roberts et al (1997) ($C_3=2.6$) which applies for $F > 20$ and $x/dF > 9$. The title of each panel shows the Froude number and C_3 constant determined from the data for each flow rate.

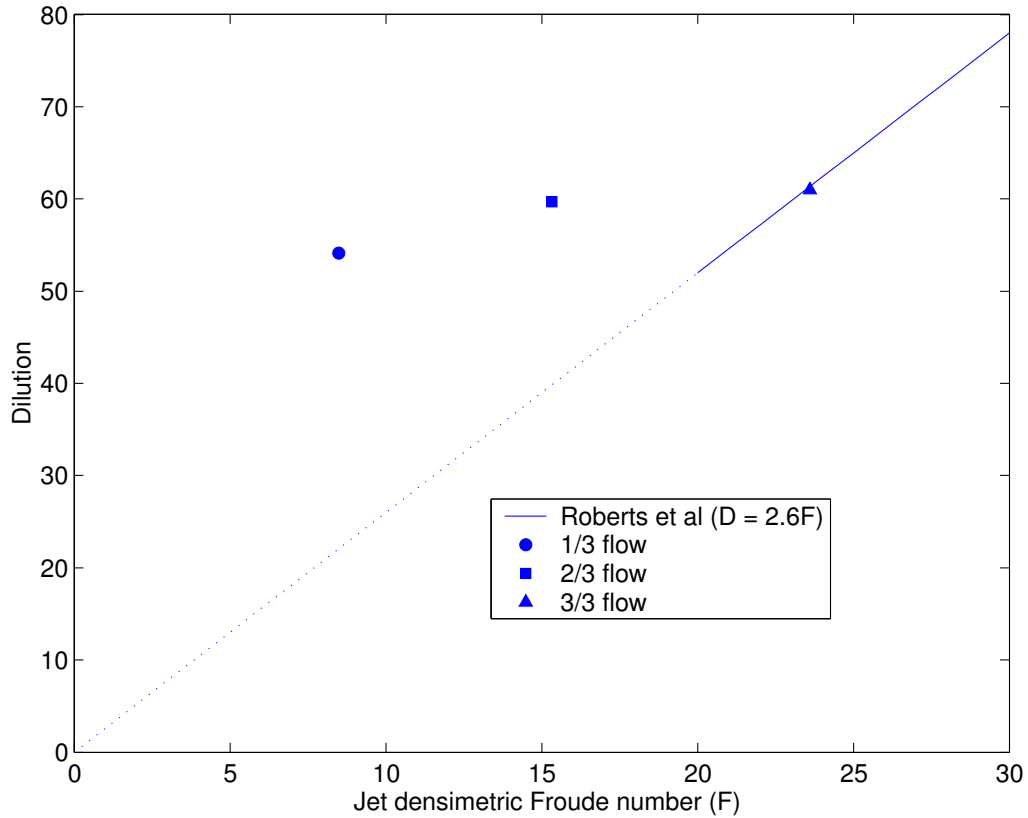


Figure 6.2. Comparison of measured dilution for the three flow rates compared to the laboratory results of Roberts et al (1997). The solid line represents the region over which the results of Roberts et al (1997) apply (ie $F > 20$), the dashed line is an extrapolation of that relationship for $F < 20$.

7 Conclusions

Based on these field measurements, the following conclusions can be drawn:

1. For $F > 20$, the dilution of the plume acts as expected based on the laboratory results of Roberts et al. (1997). For $F < 20$, the dilution at the edge of the mixing zone was found to be greater than that predicted by extrapolating the results of Roberts et al (1997).
2. Dilution at the edge of the mixing zone was found to be 54 times for the 1/3 flow, 59.5 times for the 2/3 flow, and 61.4 times for the full flow.
3. The presence of background currents modifies brine dilution, which is increased when the jet acts with the current and decreased when the jet acts against the current.
4. The maximum single dilution observed was approximately 80 times. At the concentrations during the full flow case, this results in a plume ~0.4 psu more saline than the ambient water (see Figure 5.10) at the edge of the mixing zone. Further dilution after this point is provided by environmental mixing processes.

8 References

Roberts, P. J. W. and G. Toms. 1987. "Inclined Dense Jets in Flowing Current", J Hydraulics Div, ASCE, Vol 113, No 3, March 1987. 323-341.

Roberts, P. J. W., A. Ferrier and G. Daviero. 1997. "Mixing in Inclined Dense Jets", J Hydraulics Div, ASCE, Vol 123, No 8, August 1997. 693-699.